FT-IR Spectroscopic Studies on Reorientation of Ferroelectric Liquid Crystals in a Thermoreversible Gel Network

J. Prigann,[†] Ch. Tolksdorf,[‡] H. Skupin,[†] R. Zentel,[‡] and F. Kremer*[,†]

Department of Physics, University of Leipzig, Linnestrasse 5, D-04103 Leipzig, Germany; and University of Mainz, Duesenbergweg 10−14, D-55099 Mainz, Germany

Received December 5, 2000; Revised Manuscript Received January 29, 2002

ABSTRACT: Time-resolved FTIR spectroscopy with polarized light is employed to study structure and mobility of chiral liquid crystals in mixtures with thermoreversible gels of different concentration (≤ 2 mass %). The formation of the gel stabilized structure and orientation of the liquid crystals while maintaining—for gel former concentration ≤ 1 mass %—its mobility comparable to the pure compound. Applying an external electric field during the formation of the gel enables us to imprint a preferred orientation of the liquid crystals in the mixture. This results in a memory effect similar to that observed in liquid crystalline elastomers.

Introduction

Structure and orientation of liquid crystals (LC) moieties can be stabilized by means of polymeric systems. This is for instance realized in polymer-dispersed liquid crystals (PDLC)[1−4] where microdroplets of LC molecules are immersed in a polymer network. Another approach is LC−elastomers in which the mesogenic moieties are covalently bonded to the polymeric network.[5−11] A further possibility is physically cross-linked gels, which form thermoreversible networks based on hydrogen bonding.[12,13] It is the intention of this study to analyze structure and mobility of LC molecules incorporated in such systems.

Experimental Section

Materials and Sample Preparation. For our studies, we mixed gel former with ferroelectric liquid crystals (FLC) in order to obtain a physical network with liquid crystalline units, which can be fast reoriented by external electric fields. The chemical structure and the phase transition temperatures of the ferroelectric liquid crystal (FLC) and the gel former are presented in Figure 1. The synthesis of the gel former and of the FLC molecules is described in ref 12 and in refs 14 and 15 respectively. The FLC gels with different amounts of gel former are prepared by dissolving the gel former together with pure FLC in chloroform. The mixture was heated for 3 days in a vacuum in order to remove the solvent. The phase transition temperatures were measured with DSC and polarizing microscopy for the gel former concentrations studied here (0.5, 0.75, 1, and 2 mass %). All gel mixtures show the same three phases, crystalline 52 °C, SmC* 81 °C, and isotropic, whereby with increasing gel former concentration the clearing point slightly decreased (to 80 °C for gel with 2% gel former). In contrast to pure FLC, the gel mixtures can be undercooled in the SmC* phase down to 36 °C.

The infrared measurements are performed with a cell consisting of two CaF_2 windows. Each window is coated with an indium tin oxide (ITO) layer that serves as an electrode. These windows are transparent in visible light and in IR light (down to 1000 cm^{-1}). Poly(ethylene terephthalate) (PET) foil with a thickness of 3 μm was used as spacer between the electrodes. The cell was filled with the isotropic gel by capillary forces through the gap between the windows. The sample was slowly cooled (1 °C/min) to the SmC* phase at 55 °C. Shearing between the two cell windows induced the orientation of the sample. The orientation process is supported by an external electric DC field ($E = -15.2 \times 10^4$ V/cm). To protect the (ITO) electrodes from short circuits during shearing an additional SiO_x layer is deposited on the ITO layer.

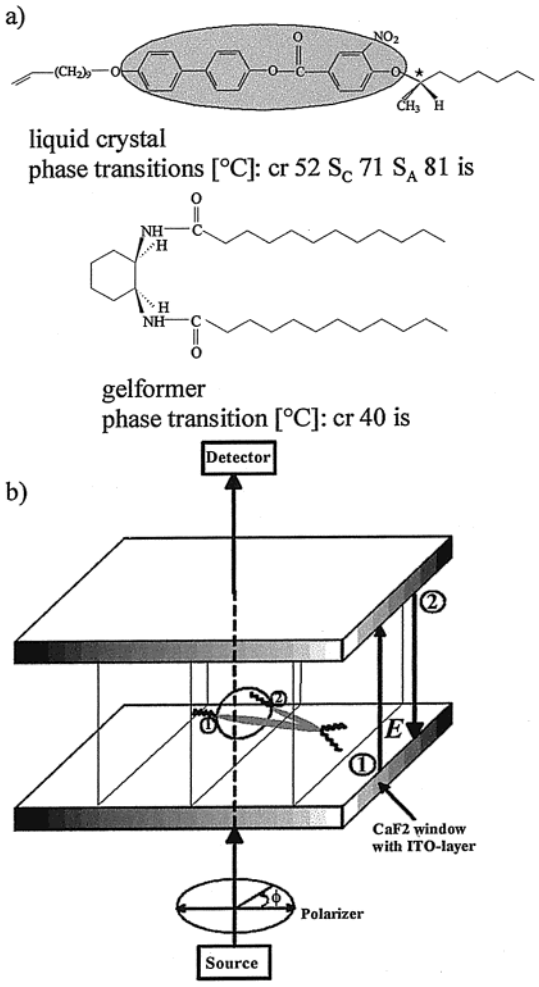

Figure 1. (a) Chemical structure and transition temperatures for the investigated liquid crystal and gel former. (b) Experimental setup: a mesogen and the aliphatic tails are sketched for the plus polarity (1) and for the negative polarity (2) of the external electric field.

[†] University of Leipzig.
[‡] University of Mainz.

10.1021/ma002065s CCC: $22.00
Published on Web 04/06/2002

Table 1. Assignment of the Investigated Bands for the Pure FLC Sample and the Gel Mixtures

vibration	molecular assignment	frequency (cm^{-1})
$\nu(C-C)_{ar}$	aromatic stretching vibration of the benzene rings of the mesogen	1614 and 1498
$\nu(C=O)$	C=O stretching vibration of the carbonyl of the mesogen	1736
$\nu_{as}(N-O)$	asymmetric N−O stretching vibration of the nitro group of the mesogen	1536
$\nu_{as}(CH_2)$, $\nu_s(CH_2)$	asymmetric and symmetric CH_2 stretching vibration of the alkyl tail of the LC	2929 and 2856

Table 2. Assignment of the Investigated Bands for the Gel Former

vibration	molecular assignment	frequency (cm^{-1})
$\nu(C-C)_{ar}$	C−C stretching vibration of the cyclohexane	1639
$\nu(C=O)$	C=O stretching vibration of the amide group	1717
$\nu_{stretch}(N-H)$	amide I vibration of the amide group	3280
$\nu_{deform}(N-H)$	amide II vibration of the amide group	1545
$\nu_{as}(CH_2)$, $\nu_s(CH_2)$	asymmetric and symmetric CH_2 stretching vibration of the alkyl tail of the LC	2929 and 2856

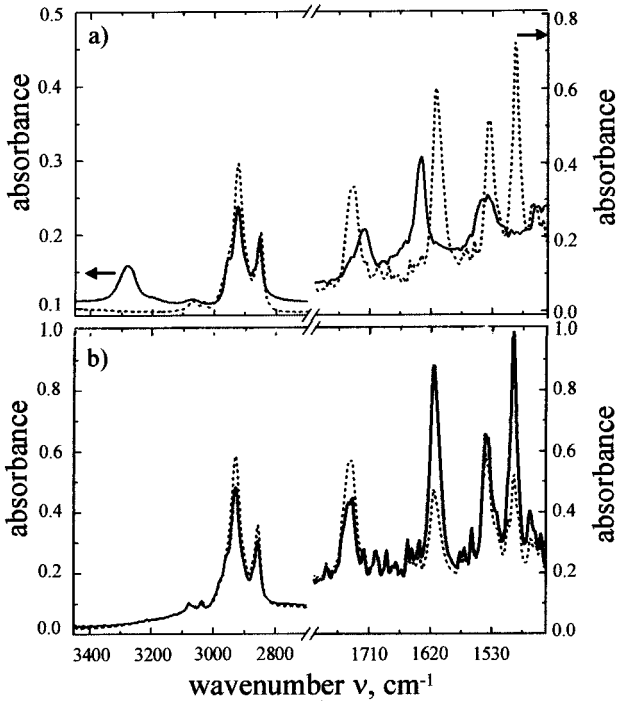

Figure 2. Infrared absorbance spectra (a) of the gel former (solid line) and the pure ferroelectric liquid crystal (dashed line) and (b) of the gel mixture with 0.75% gel former for polarizer angle $\phi = 0°$ (solid line) and for polarizer angle $\phi = 90°$ (dashed line).

Measurement Technique. An FTS-6000 FT-IR (Bio-Rad) spectrometer accomplished with an IR microscope (UMA-500, Bio-Rad) is used to record the IR spectra. For the IR measurements, regions of uniform orientation (100 × 100 μm^2) were selected. The IR microscope allows studying these measurement spots also in visible light with crossed polarizers. The polarized IR beam propagates perpendicular to the plane of the cell windows (Figure 1). The IR spectra are measured in dependence on the polarizer angle ϕ from 0 to 180° in steps of 10°. The polarizer consists of a KRS5-crystal with an evaporated gold lattice on top and a programmable stepper motor.

For static measurements the IR spectra are recorded with a spectral resolution of 4 cm^{-1} in the rapid scan mode of the FTS-6000. To obtain information about the response to an external electric field of the sample, time-resolved FT-IR spectra are collected. By use of the step−scan technique described earlier,[16] spectra are recorded with a resolution in time of 5 μs and a spectral resolution of 8 cm^{-1}. The IR spectra of the pure FLC and the gel former are compared (Figure 2a) and the band assignments are given in Tables 1 and 2. The good orientation of the FLC is proven by the strong dichroism of the sample. The gel former is not detectable in the IR spectra of the 0.75 mass % gel mixture (Figure 2b) because of its low concentration.

Results and Discussion

Static Measurements. Detailed information about the average orientation and the orientational order of the different molecular segments in the liquid crystalline (gel) samples can be obtained (Figure 3) from the polarizer dependent absorbance of the corresponding bands $A_\nu(\phi)$.

The absorbance A_ν of a band centered at ν is in first approximation proportional to $A_\nu \sim \langle(\epsilon\mu)^2\rangle$ for infinite thick films,[17] where ϵ is the polarization vector of the IR light; $\mu = (\mu_x, \mu_y)$ is the transition moment vector of the corresponding band and the brackets $\langle\ \rangle$ denote the average over the measurement spot. For the measurements presented here, the polarization vector is rotated within one plane perpendicular to the IR beam (*z*-axis in the laboratory system) and is described by

$$\epsilon = |\epsilon|\ (\cos\phi, \sin\phi) \tag{1}$$

This leads to

$$A(\phi) \sim \langle(\epsilon\mu)^2\rangle = |\epsilon|^2\ (\langle\mu_x^2\rangle \cos^2\phi + \langle\mu_y^2\rangle \sin^2\phi)$$

and this equation can be fitted[14] by

$$A(\phi) \sim a + b\cos(2(\phi - \phi_0)) \tag{2}$$

where f_0 is the polarizer angle for which maximum absorbance is obtained. The values a, b, and ϕ_0 are dependent on the distribution function of the transition moment μ and hence on the average orientation and the orientational order of the corresponding segment.

For the 0.75% gel mixture under application of three different electric dc field strengths, Figure 3 shows the $A(\phi)$ dependence of several bands as polar plots. The absorbance A is extracted from the amplitude of the band at its center with respect to an appropriate baseline. The data are fitted according to

$$A'(\phi) = \log A(\phi) = -\log(a\ 10^{-b\cos(2(\phi-\phi_0))}) \tag{3}$$

which is deduced from eq 2 under consideration of the finite thickness of the sample.[18] For a transition moment parallel to the long axis the dichroic ratio is $R = (-\log a + b)/(-\log a - b)$. The angle ϕ_0 is a measure for the average orientation of the transition moment in the projection plane normal to the IR propagation and describes an "apparent orientation" of the corresponding molecular segment. For all bands ϕ_0 is determined from the mathematical fit (eq 3) with a precision ≤1°.

Comparing the influence of the static external electric field $\boldsymbol{E}$ (Figure 3a−c) on the orientation delivers the following features: (i) The mean orientation (Table 3)

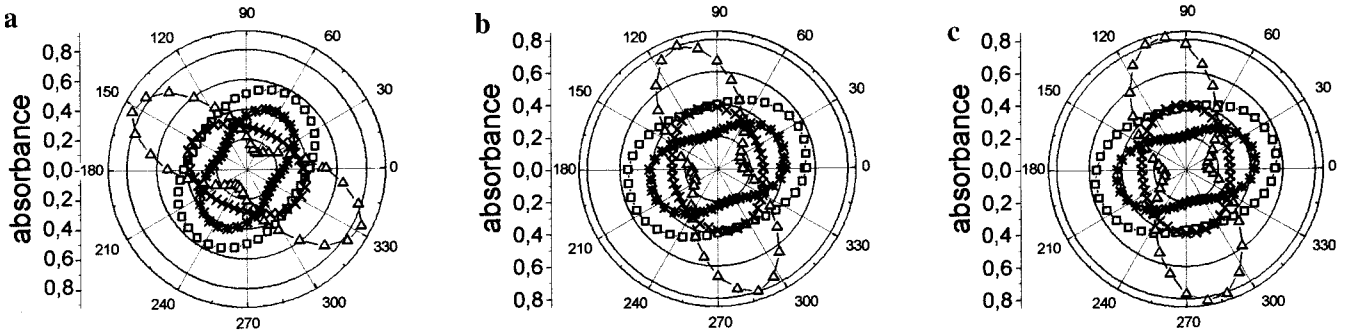

Figure 3. Polar plot of the polarizer-dependent absorbance for the CH_2 group (-□-), the C═O group (-∗-), the phenyl group (-△-) and the NO_2 group (-×-) of the gel mixture with 0.75% gel former under the influence of an external static electric field of $+21.7 \times 10^4$ (a), 0 (b), and -21.7×10^4 V/cm (c) in the SmC* phase (55 °C). The lines are the mathematical fit. The experimental error in the absorbance is less than the symbol size.

Table 3. Dichroic Ratio *R* and the Angle f_0 of the Investigated Bands for the Three States of External Dc Field

	$E = +21.7 \times 10^4$ V/cm		$E = 0$ V/cm		$E = -21.7 \times 10^4$ V/cm	
	R	ϕ_0	R	ϕ_0	R	ϕ_0
meosgen group	6.55	150.4	6.0	109.8	6.52	98.5
carbonyl group	1.72	59.2	1.69	20.1	1.72	9
CH_2-group	1.49	59.4	1.46	21	1.49	10.1
nitro group	1.46	156.4	1.39	105.3	1.46	92.3

of the mesogenic core is not symmetric with respect to ***E***. This reflects a memory effect due to a negative dc bias field, which was present during gelation. (ii) From the dichroic ratio $R = A(\phi_{max})/A(\phi_{min})$ for the mesogen, the order parameter can be deduced according to

$$S = (R - 1)/(R + 2) \tag{4}$$

Its high value ($S = 0.74$) proves the good orientation of the liquid crystalline system in the gel. (iii) The mean orientation of the NO_2 groups is not parallel to the director and its dichroic ratio is comparably small (Table 3). This is a proof for the biased rotation of the NO_2 group around the long axis, i.e., an asymmetry of the dipolar distribution function around the mesogenic axis.[18−22] (iv) Due to the chemical structure of the FLC, the C═O groups have a transition moment which is oriented perpendicular to the mesogenic axis. (v) The aliphatic CH_2 groups have, because of their zigzag orientation, a small dichroic ratio and a mean orientation perpendicular to the long axis.

The angle ϕ_0 (phenyl, NO_2 group) and the angle $\phi_0 + 90°$ (CO, CH_2 group) were also measured for lower dc field strengths and are presented in Figure 4. The plot shows clearly that a strong E field (E_{st} in Figure 4) is necessary to overcome the elastic forces of the gel network to reach the nonstabilized state of the liquid crystal molecules (asymmetric behavior). The larger angular excursion of the NO_2 group is caused by the biased rotation of its polar group around the long axis of the molecule.

Dynamic Measurements. To gain information about the dynamics of the different molecular moieties (reorientation time, reorientation angle, reorientation path, synchronicity), time-resolved FT-IR spectra are collected at a complete set of polarizer angles ϕ. The sample was switched with a rectangular pulsed field of a frequency of 4000 Hz and field strength of $\pm 15.2 \times 10^4$ V/cm. From the time-resolved FT-IR spectra, the polarizer dependent absorbance $A(\phi)$ is extracted in time intervals of $\Delta t = 5$ μs for all bands under study. This enables us to

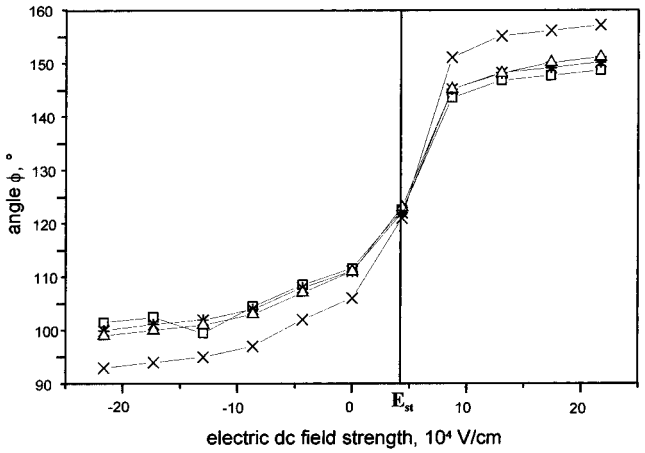

Figure 4. Electric dc field strength dependence of the angle ϕ_0 for the CH_2 group (-□-), the C═O group (-∗-), the phenyl group (-△-) and the NO_2 group (-×-) of the gel mixture with 0.75% gel former. The measurements are carried out starting with an electric field of $+21.7 \times 10^4$ V/cm and ending with an electric field of -21.7×10^4 V/cm. The lines are guides for the eyes. The experimental error in the absorbance is less than the symbol size.

obtain the angle ϕ_0 in the same way as described for the static measurements. Figure 5 shows the time evolution for the different molecular moieties of the gel mixture with 0.75% gel former. The reorientation starts immediately after reversion of the electric field polarity. Within each half of a switching period the angle ϕ_0 of all vibration bands reaches a plateau. The value before inversion of the polarity takes place is called ϕ_1, while ϕ_2 is the corresponding value after the orientation is completed. The NO_2 group shows the largest change ($\Delta\phi = \phi_2 - \phi_1$) in the angular excursion: $\Delta\phi(NO_2) = 64°$, the angle for the other groups are smaller: $\Delta\phi$(phenyl) $= 51°$, $\Delta\phi$(C═O) $= 42°$, and $\Delta\phi(CH_2) = 38°$. This observation is in accord with the findings from the static measurements (Figure 4).

To compare the reorientation time of different molecular moieties, the normalized angles ϕ_N were calculated as follows:

$$\phi_N = (\phi(t) - \phi_1)/\Delta\phi \tag{5}$$

The results are plotted in the inset of Figure 5. As can be seen from this figure, the normalized curves for all bands coincide with each other within the limits of experimental accuracy of ±1°.

The memory effect—caused by the electrical field present during gel formation—shows up in the difference

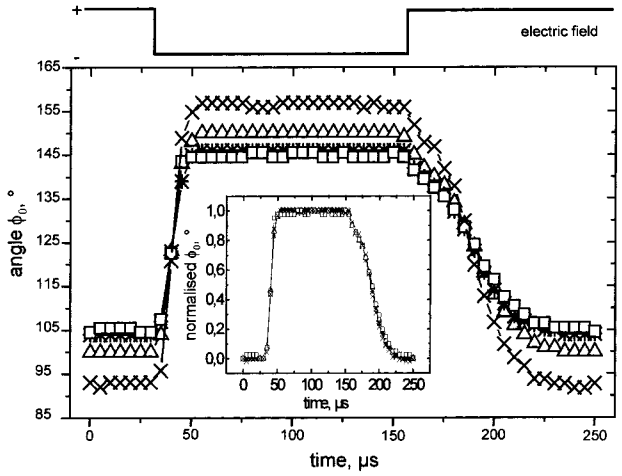

Figure 5. Time-resolved angles $\phi_0(t)$ for the CH_2 group (-□-), the C═O group (-∗-), the phenyl group (-△-) and the NO_2 group (-×-) of the gel mixture with 0.75% gel former under an influence of an electric field of $\pm 15.2 \times 10^4$ V/cm and frequency 4 kHz at 55 °C. The normalization of $\phi_0(t)$ shown in the inset reveals the synchronous reorientation of the different molecular moieties. The lines are guides for the eyes. The experimental error in the absorbance is less than the symbol size. The switching of the electric field strength is shown on the top of Figure 5.

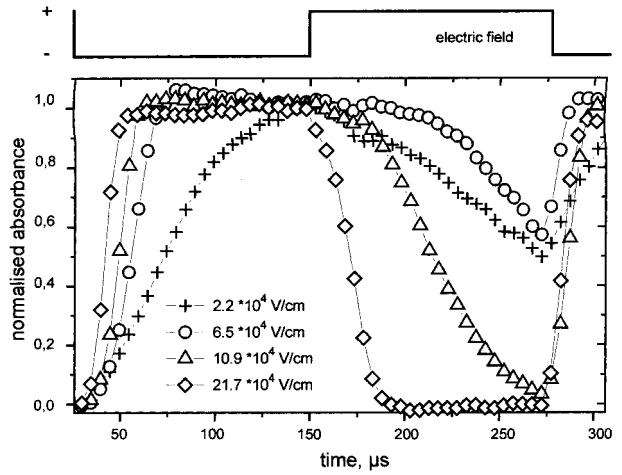

Figure 6. Time-resolved normalized absorbance of the mesogenic absorption band $\nu = 1614$ cm^{-1} for the electric field strength: 2.2×10^4 V/cm (-+-), 6.5×10^4 V/cm (-○-), 10.9×10^4 V/cm (-△-) and 21.7×10^4 V/cm (-◇-) with fixed polarizer $\phi = 55°$ and at a temperature of 55 °C. The lines are guides for the eyes. The experimental error in the absorbance is less than the symbol size. The increase of the normalized absorbance at time $t = 275$ μs is caused by the third switching impulse. The time evolution of the electric field strength is shown on the top of Figure 6.

of the switching times after applying electrical field from positive to negative direction and vice versa (Figure 5); it proves the energetic preference of the imprinted orientation. This appears as well in the field strength dependence of the time evolution after switching (Figure 6). As expected the reorientation times of the mesogen depend also strongly on the gel former concentration (Figure 7). This is observed in the angular excursion of the mesogens during switching (Figure 8) too in accordance with electrooptical measurements.[23]

Conclusions

Thermoreversible gels with different network densities are prepared by mixing a gel former with a low molecular chiral liquid crystalline compound in a solvent. The gel former stabilizes the orientation of the liquid crystals but enables for concentration ≤ 1 mass % a reorientational dynamics comparable the pure system.

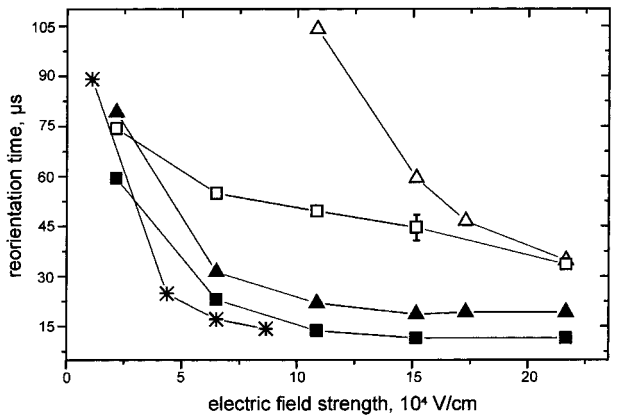

Figure 7. Reorientation time vs the applied electric field strength: solid symbols, switching from nonstabilized to stabilized state; open symbols, switching from stabilized to nonstabilized state; -□-, gel mixture with 0.5% gel former; -△- gel mixture with 0.75% gel former; -∗- pure liquid crystal. The lines are guides for the eyes.

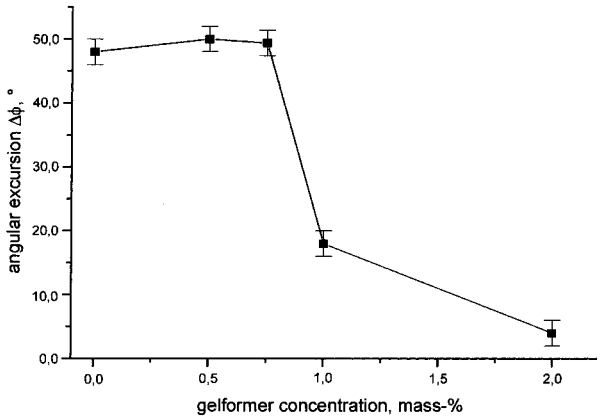

Figure 8. Angular excursion $\Delta\phi$ on dependence of gel former concentration for a fixed electric field of $\pm 15.2 \times 10^4$ V/cm. The lines are guides for the eyes.

Acknowledgment. Support by the German Science Foundation within the framework of the Sonderforschungsbereich 294 is highly appreciated.

References and Notes

(1) Fergason, J. L. Encapsulated liquid crystal and method. US Patent 4,435,047, 1984.
(2) Doane, J. W.; Vaz, N. A.; Wu, B.-G.; Sumer, S. *Appl. Phys. Lett.* **1986**, *48*, 269−271.
(3) Doane, J. W.; Chidishimo, G.; Vaz, N. A. Light modulating material comprising a liquid crystal dispersion in a plastic matrix. US Patent 4,688,900, 1987.
(4) Stannarius, R.; Crawford, G. P.; Chien, L. C.; Doane, J. W. *J. Appl. Phys.* **1991**, *70*, 135−143.
(5) Skupin, H.; Kremer, F.; Shilov, S. V.; Stein, P.; Finkelmann, H.; *Macromolecules* **1999**, *32*, 3746−3752.
(6) Brehmer, M.; Zentel, R.; Giessmann, F.; Germer, R.; Zugenmaier, P. *Liq. Cryst.* **1996**, *21*, 589−596.
(7) McArdle, C. B. Side Chain Liquid Crystal Polymers; Blackie and Son; Glasgow, Scotland, 1989.
(8) Zentel, R. *Angew. Chem., Int. Ed. Engl. Adv. Mater.* **1989**, *28*, 1407.
(9) Semmler, K.; Finkelmann, H. *Polym. Adv. Technol.* **1994**, *5*, 231.

(10) Semmler, K.; Finkelmann, H. *Macromol. Chem. Phys.* **1995**, *196*, 3197.
(11) Eckert, T.; Finkelmann, H.; Keck, M.; Lehmann, W.; Kremer, F. *Macromo. Rapid Commun.* **1996**, *17*, 767.
(12) Kato, T.; Kondo, G.; Hanabusa, K. *Chem. Lett.* **1998**, 193−194.
(13) Hanabusa, K.; Yamada, M.; Kimura, M.; Shirai, H. *Angew. Chem.* **1996**, *108*, 2086−2088.
(14) Part I: Gebhard, E.; Zentel, R. *Macromol. Chem. Phys.* **2000**, *201*, 902−910.
(15) Part II: Gebhard, E.; Zentel, R. *Macromol. Chem. Phys.* **2000**, *201*, 911−922.
(16) Shilov, S.; Skupin, H.; Kremer, F. In *Liquid Crystal: Physics, Technology and Applications*; Rutkowska, J.; Ed.; *Proceedings of SPIE* 3318, SPIE: Bellingham, WA, 1998, pp 62−67.
(17) Zbinden, R. Infrared Spectroscopy of High Polymers; Academic Press: London; 1964; Chapter 5.
(18) Hide, F.; Clark, N. A.; Nito, K.; Yasuda, A.; Walba, D. M. *Phys. Rev. Lett.* **1995**, *75*, 2344−2347.
(19) Verma; et al. *Phys. Rev. E*. **2001**, *63*, 1704-.
(20) Shilov, S.; Gebhard, E.; Skupin, H.; Zentel, R.; Kremer, F. *Macromolecules* **1999**, *32*, 1570−1575.
(21) Skupin, H.; Shilov, S.; Kremer, F.; Gebhard, E.; Zentel, R. *Mol. Cryst. Liq. Cryst.* **2001**, *358*, 37−51.
(22) Koden, M.; Kuratate, T.; Funada, F.; Awane, K.; Sakaguchi, K.; Shiomi, Y. *Mol. Cryst. Liq. Cryst. Lett.* **1990**, *7*, 79.
(23) Tolksdorf, Ch.; Zeniel, R. *Adv. Mater.* **2001**, *13*, 1307−1310.

MA002065S